International Journal of Physics and Applications
Online ISSN: 2664-7583; Print ISSN: 2664-7575; Impact Factor: RJIF 5.22
Received: 06-07-2020; Accepted: 21-07-2020; Published: 07-08-2020
www.physicsjournal.in
Volume 2; Issue 2; 2020; Page No. 03-05

Analysis of spherical propagation models for multipath-propagation predictions

Priyaranjan
Research Scholar, Department of Physics, J.P. University, Chapra, Bihar, India

Abstract
Multipath fading leads to a limitation in the availability and/or reliability of microwave links. In this paper is study the propagation mechanism under fading conditions propagation models, based on ray theory, above a spherical earth have been developed and compared to the well-known planar propagation model above a "flattened eartha"
The models are shown, including an accuracy analysis, and the use of spherical propagation models is illustrated for surface duct layers above water.

Keywords: spherical propagation models, multipath-propagation predictions

Introduction
Radio propagation is the behaviour of radio wave when they are transmitted, or propagated from one point on the Earth to another, or into various parts of the atmosphere.
Radio propagation is affected by the daily changes of water vapor in the troposphere and ionization in the upper atmosphere, due to the Sun. Understanding the effects of varying conditions on radio propagation has many practical applications, from choosing frequencies for international shortwave broadcasters, to designing reliable mobile telephone systems, to radio navigation, to operation of radar systems.
Radio propagation is also affected by several other factors determined by its path from point to point. This path can be a direct line of sight path or an over-the-horizon path aided by refraction in the ionosphere, which is a region between approximately 60 and 600 km. Factors influencing ionospheric radio signal propagation can include sporadic-E, spread-F, solar flares, geomagnetic storms, ionospheric layer tilts, and solar proton events.
Radio waves at different frequencies propagate in different ways. At extra low frequencies (ELF) and very low frequencies the wavelength is very much larger than the separation between the earth's surface and the D layer of the ionosphere, so electromagnetic waves may propagate in this region as a waveguide. Indeed, for frequencies below 20 kHz, the wave propagates as a single waveguide mode with a horizontal magnetic field and vertical electric field. The interaction of radio waves with the ionized regions of the atmosphere makes radio propagation more complex to predict and analyze than in free space. Ionospheric radio propagation has a strong connection to space weather. A sudden ionospheric disturbance or shortwave fadeout is observed when the x-rays associated with a solar flare ionize the ionospheric D-region. Enhanced ionization in that region increases the absorption of radio signals passing through it. During the strongest solar x-ray flares, complete absorption of virtually all ionospherically propagated radio signals in the sunlit hemisphere can occur. These solar flares can disrupt HF radio propagation and affect GPS accuracy.
Predictions of the average propagation conditions were needed and made during the Second World War. A most detailed code developed by Karl Rawer was applied in the German Wehrmacht, and after the war by the French Navy.

Theory
In the model with planar earth (Figure 1) the vertical refractive index profile m is assumed to be dependent on z only and is characterized by the transformation

$$\frac{dn(r)}{dr} = \frac{dm(z)}{dz} = \frac{1}{R_a} = B^n = \frac{1}{R_a}$$

Where n= refractive index in the spherical model with earth radius R_s and with assumed radial dependency r
r_1 = refractive index in the planar model
B^n = refractive index gradient per meter in the planar model

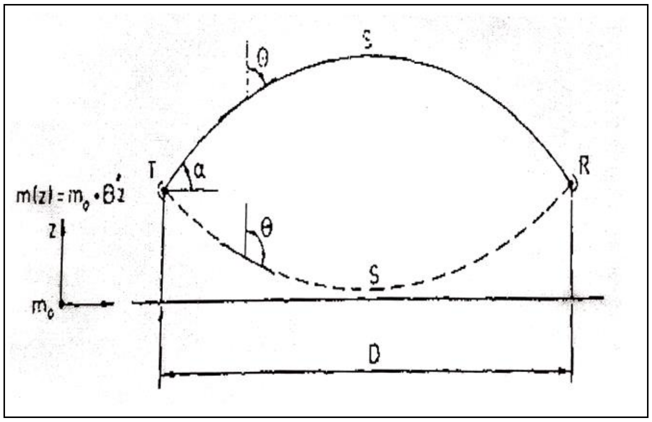

Fig 1: Planar propagation model

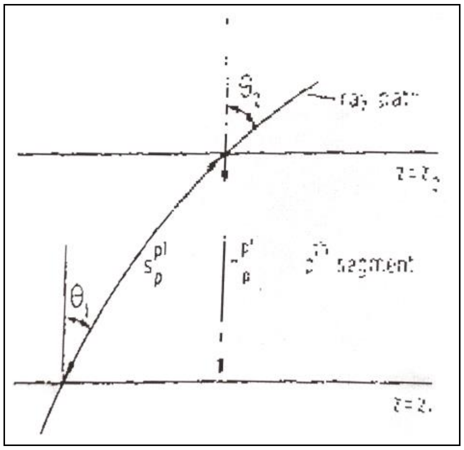

Fig 2: Ray parameters in planar propagation model

Segmentation is carried out in such a way that B" = constant per segment p (Figure 2). The ray parameters are functions of the refractive index profile and θ. In the planar model the ray parameters per segment become
-h_p^{pl} = height difference of the ray = segment thickness
-d_p^{pl} = horizontal distance of the ray along the earth surface
-s_p^{pl} = path length of the ray
-t_p^{pl} = path delay of the ray
If a ray reaches a maximum or minimum height within the segment an extra segment is introduced based on these heights. The whole radio path is described by summing the ray parameters.

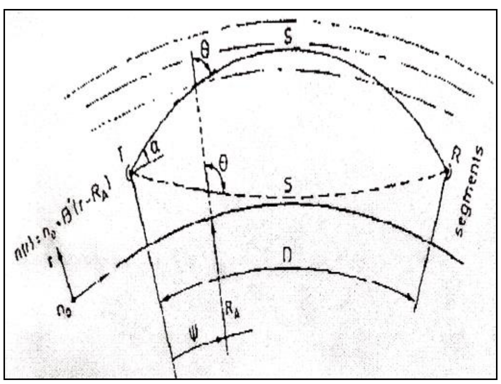

Fig 3: Spherical propagation model

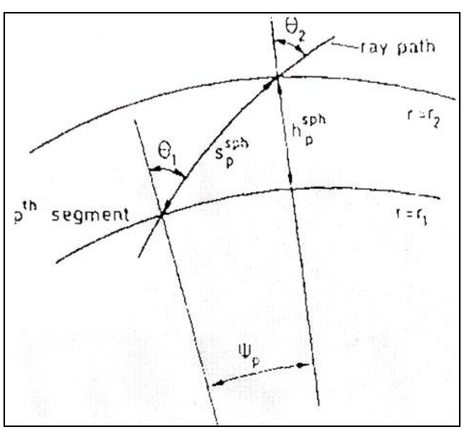

Fig 4: Ray parameters in spherical propagation model

In the model with spherical earth (Figure 3) the refractive index profile is characterized by the transformation

$$\frac{dn(r)}{dr} = \frac{dN(r_f)}{dr_f} - \frac{1}{R_a} + \frac{1}{R_f} = B' - \frac{1}{R_a} + \frac{1}{R_f}$$

Where N = refractive index in the spherical model with arbitrary fictive radius R_f
B' = refractive index gradient per meter in the spherical model
Segmentation is illustrated in Figure 4 where B' a constant per segment p. The ray parameters in the spherical model become
-h_p^{spn} = segment thickness
-$d_p^{spn} = r_f.\Psi_p$ = horizontal distance of the ray along the earth surface -S_p^{spn} = path length of the ray
-t_p^{spn} = path delay of the ray
Different analytical approximations for the ray parameters have been derived for B'>-N ($_{rf}$) / r_f B' <-N (r_f)/r_f and for the rays which reach maximum heights. Per segment analytical expressions can be obtained by making approximations in the ray theory, especially of the term

$$I = \sqrt{r_f^2 N^2(r_f) - c^2}$$

Using Snell's law for as spherical layered medium the ray path constant C becomes
c=N (r_f) •$r_{f.}$ sinθ
For B'<–N (r_f)/r_f the term I yields

$$I = \sqrt{(r_m^2 - r_f^2)k_p}$$

r_m is the maximum r_f value the ray would reach if the refractive index gradient B'_p = constant were extended to above. This means $r_m > r_2$. The factor K_p is chosen so that for $r_m > r_2$
$(r_m^2 - r_2^2)\, k_h = r_2^2 N^2\,(r_2) - C^2$
And for $r_m = r_2$
$K_p = -N^2\,(r_1) - B'_p.\ N\,(r_1).r_1$
For B'>-N'r_f)/r_f the term I yields

$$I = \sqrt{k_p^{'}(k_f^2 - r_1^2) + k_p^n}$$

K'_p and K''_p are chosen so that the approximation is optimal for $r_f = r_1$; K'_p and K''_p become
$K'_p = -N^2\,(r_1) - B'_p \cdot N\,(r_1).r_1$
$K''_p = -N_2\,(ri).r_1^2 - c^2$
An application of the theory is given for a refractive index profile characteristic of a duct above water. This model has been chosen because strong gradients and thus strong convergence or divergence of the rays can be expected just above the water surface. At the same time, there is the possibility to investigate whether u simple relationship exists between the amplitude of incoming rays and their delay time.
For the microwave link, the following is selected:
– Distance between transmitter and receiver = 40 km
– Antenna heights = 80 m

The modified logarithmic refractive index profile above a flattened earth is given by (Figure 5).

$$M(z) = C_2\left[z - z_1 - (d + z_2) \bullet in\left(\frac{z+z\,0}{z_1 + z_0} \right)\right] + M_1$$

Where
d = duct height (5–50 moters)
Z_0 = roughness parameter at the earth's surface (10^{-3}m)
Z_1 = height where M (Z_1) =H_1 and C_2 = characterizes dM/dz at high altitudes (s > 3d).

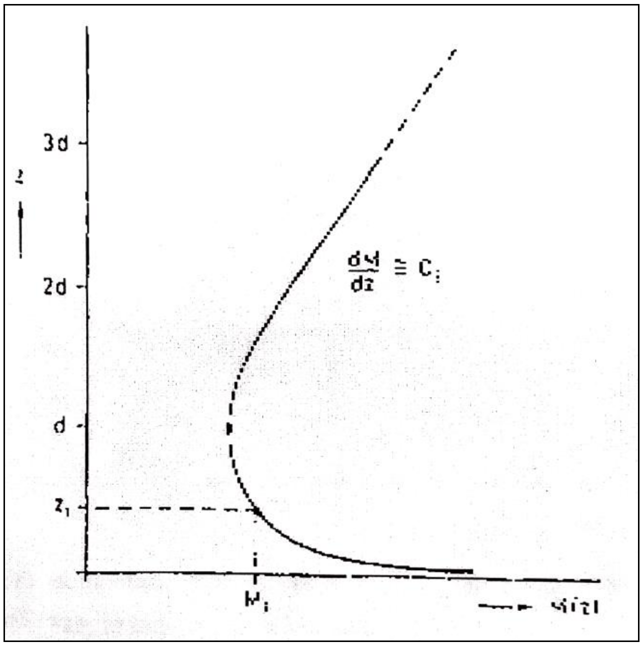

Fig 5: Modified logarithmic refractive index profile above a planar earth

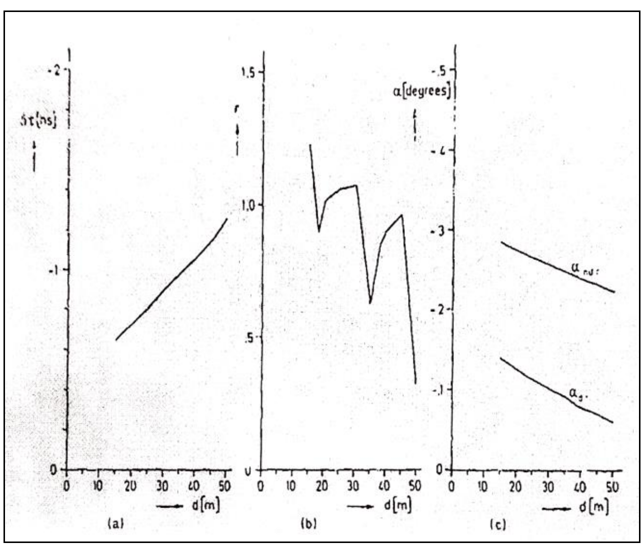

Fig 6: computational results as function of duct height d. Modul. 1: k=1, M_1 – 325; a) time delay differenceδτ: b) relative amplitude of the indirect ray: c) angles of arrival.

The refractive index n above the spherical earth is determined by:

$$M(z) = (n - 1 + \frac{z}{R_a}) \rightarrow \quad dM/dz = (dn/dz + 1/R_a)\ 10^6$$

Where dn/dz = refractive index gradient above a spherical earth with earth radius R_a for a fictive earth radius = $R_{F=}kR_a$ it is found that:

$$R_f = \frac{1}{(dn/dz) + 1/R_a} = dM/dz = \frac{10^s}{kR_a} = C_2 \text{ for } z>3d$$

This means that K determines the model conditions for high altitudes. The computations with 1 meter segmentation and for K= 1, 4/3 (standard atmosphere above the duct) and K = 2, are presented in Figures 5 and 6. In these figures δ_t is the delay time difference and r is the relative amplitude factor of the two rays in this two-way propagation model

A dominant k-dependency on δ_t and a clear correlation between δ_t and a are found as a function of the duct height, while no simple relationship exists between δt and r.

Conclusion

In this paper, the accuracy analysis shows strong convergence in path delay results by decreasing segment thicknesses. The example of a two-way spherical model based on surface duct layers above water indicates a strong relationship between time delay differences and angles of arrival combined with a dominant dependency of the model on the time delay computations.

References

1. Turin GL. 'Communication through noisy', random–multipath channels IRE Convention Record, pars 4, 1956, 154-566.
2. Turjn GL, Clapp FD, Jonston TL, Fine SB, Lavry D. A Statistical model of urban multipath propagation, IEE Trans. Veh. Technol. 1972; 21:1-9.
3. Hashemi H. 'Simulation of the urban radio propagation channel', IEEE Trans. Vets, Technol, 1979, 213-224.
4. Bajwa AS. 'UIFF' wideband statistical model and simulation of mobile radio multipath propagation effects', IEE Proc. F. 1985; 132(5):327-333.
5. Rappaport TS, Seidel SY, Sings R. '900 MHz multipath propagation measurements for US digital cellular radio telephone', IEEE Trans. Felt. Technol. 1990; 39(2):132-139
6. Sales AAM, Velenzuela RA. 'A Statistical model for indoor multipath propagation'. IEEE J Sal Areas Commun. 1987; 5(2):128-137.
7. Hashemi H, Tholl D, Morrison C. 'Statistical modelling for the indoor radio propagation channel: pact I'. Proc. IEEE Vehicular Technology Conference, VTC'92. Denver, Co, 1992, 338-342.